Nanolithography probes

Novel Ultrananocrystalline Diamond Probes for High-Resolution Low-Wear Nanolithographic Techniques

Keun-Ho Kim, Nicolaie Moldovan, Changhong Ke, Horacio D. Espinosa, Xingcheng Xiao, John A. Carlisle, and Orlando Auciello*

***A** hard, low-wear probe for contact-mode writing techniques, such as dip-pen nanolithography (DPN), was fabricated using ultrananocrystalline diamond (UNCD). Molding within anisotropically etched and oxidized pyramidal pits in silicon was used to obtain diamond tips with radii down to 30 nm through growth of UNCD films followed by selective etching of the silicon template substrate. The probes were monolithically integrated with diamond cantilevers and subsequently integrated into a chip body obtained by metal electroforming. The probes were characterized in terms of their mechanical properties, wear, and atomic force microscopy imaging capabilities. The developed probes performed exceptionally well in DPN molecular writing/imaging mode. Furthermore, the integration of UNCD films with appropriate substrates and the use of directed microfabrication techniques are particularly suitable for fabrication of one- and two-dimensional arrays of probes that can be used for massive parallel fabrication of nanostructures by the DPN method.*

Keywords:
- AFM
- diamond
- dip-pen nanolithography
- nanocrystalline materials
- probe tips

1. Introduction

A number of scanning probe techniques have been developed in recent years. These techniques require sophisticated probes, such as those employed in nanolithography,[1–5] arrays for parallel imaging, writing, and data reading/recording,[6–8] or even more complex tasks such as drilling, cutting, or milling.[9,10] The cost of these specialized probes and their functional life, in terms of scanning distance, are strongly competing parameters in their design. Engineering new materials and developing simple fabrication processes is one way of addressing this problem. Both aspects are examined here. We also focus on probes that may be attractive for integrating new functions, such as independent sensing and actuation, arraying, multiple probing techniques, microfluidics, and/or scanning probe machining. The lifetime of probes is typically shortened by mechanical failure in operation and handling, pickup of material and particles from the samples, and wear. The former can be enhanced by more careful procedures, but the latter is especially important in contact-mode techniques, such as contact-mode AFM imaging,[11] scanning spreading resistance microscopy,[12] atomic-scale potentiometry,[13] scanning thermal microscopy,[14] and lithography,[2,15] such as dip-pen and fountain-pen nanolithography.[1–5] Hard materials are typically employed to reduce probe wear, among which diamond is the obvious material of choice. Furthermore, diamond possesses surface and bulk properties that are ideal for probes: very low chemical reactivity, a low work function when the surface is chemically conditioned, no oxide layer formation, tunable electrical conductibility by doping, and thermal conductivity ranging from relatively low ($\approx 10\,\mathrm{W\,K^{-1}\,m^{-1}}$) for ultra-

[*] K.-H. Kim,[+] Prof. N. Moldovan,[+] C. Ke, Prof. H. D. Espinosa
Department of Mechanical Engineering
Northwestern University
Evanston, IL 60208 (USA)
Fax: (+1) 847-491-3915
E-mail: espinosa@northwestern.edu
Dr. X. Xiao, Dr. J. A. Carlisle, Dr. O. Auciello
Materials Science Division
Argonne National Laboratory
Argonne, IL 60439 (USA)

DOI: 10.1002/smll.200500028

NANO MICRO small

nanocrystalline diamond (UNCD) to extremely high ($\approx$2000 $W K^{-1} m^{-1}$) for single-crystal diamond.[16]

In previous work, several species of diamond films have been employed in probe fabrication by different groups,[17–22] which vary mainly in the degree of crystallinity of the diamond. Initial attempts at producing conductive diamond probes for scanning tunneling microscopy involved boron-implanted macroscopic diamond crystals, which were machined by polishing and mechanically assembled into AFM cantilevers.[19] Later attempts used boron-doped epitaxial layers grown by chemical vapor deposition (CVD) on natural diamond in a similar fashion.[20] These approaches showed the feasibility of employing conductive diamond in probe manufacturing, but they are clearly not well-suited for integration. Micro- or nanocrystalline diamond films[21] have superior mechanical characteristics (wear, hardness) with respect to amorphous carbon or diamond-like carbon (DLC) materials,[22] but have higher surface roughness than the latter. DLC films are smoother and easier to integrate into more complex fabrication schemes but cannot be made highly conductive. Hence, micromachining techniques based on molding methods[17,18,23] were developed to minimize the major problem of crystalline diamond films, that is, their surface roughness when used as a coating on tips made of other materials such as Si. An alternative is to use thin conformal films to cover probes made of other materials. This technique has the disadvantage that it increases the initial tip radius of the probes (10–20 nm) by the thickness of the diamond film (typically 70–100 nm to achieve full coverage of the substrate); thus, it results in a much lower tip sharpness. Typical commercial diamond-coated tips have radii in the 100–200 nm range. In particular cases, nanoscale roughness features can improve the radius of the contact area, but the general shape and aspect ratio of the probes is compromised. Molding of crystalline diamond works reasonably well, but leaves the growing surface of the diamond very rough, which is unsuitable to continue the integration with other, later-deposited layers and further processes.

UNCD films,[24] with grain sizes in the 2–5 nm range, retain most of the surface and bulk properties of crystalline diamond as well as the smoothness of the substrate.[25] The material is deposited by microwave plasma-enhanced chemical vapor deposition (MPCVD) from an Ar–CH_4 (99:1) gas mixture. Table 1 shows some of the remarkable properties of UNCD, as compared to other forms of diamond. The term ultrananocrystalline diamond (UNCD) is used to distinguish this material from microcrystalline diamond (MCD),[21] nanocrystalline diamond (NCD),[26] and diamond-like carbon (DLC),[22] since UNCD exhibits the smallest grain size (except for DLC films), and different morphology and properties than all the other forms of diamond mentioned above. Due to the small size of the grains, the ratio of grain-boundary atoms (which consist of a mixture of sp^2, sp^3, and other forms of carbon bonding) to bulk atoms (sp^3) is high, which leads to interesting material properties such as a predictable fracture strength equal to or higher than that of single-crystal diamond and the ability to incorporate nitrogen into the grain boundaries which gives rise to greatly increased (up to 250 $\Omega^{-1} cm^{-1}$) room temperature n-type conductivities. A comparison between these species of diamond is given in Table 1.

The remarkable hardness of UNCD makes it the material of choice for contact-mode nanoprobe tips. Erdemir et al.[26] measured wear rates on MCD films using a SiC pin-on-disk tribometer measurement technique. They found that MCD films exhibit wear rates from 0.48×10^{-6} to 55.0×10^{-6} $mm^3 Nm^{-1}$. By contrast, UNCD films exhibit a wear rate as low as 0.018×10^{-6} $mm^3 Nm^{-1}$. It was also found that the as-grown UNCD films have friction coefficients roughly two orders of magnitude lower than those of MCD films of comparable thickness. The wear rate of a SiC pin rubbed against a UNCD film was found to be $\approx$4000 times lower than that of a SiC pin rubbed against an as-deposited MCD film.

Herein, we report the fabrication of UNCD probes for AFM, which integrate tips and cantilevers made entirely of this material, both in nonconducting (undoped) and conducting (nitrogen-doped) states. The probes were characterized by electron microscopy and resonance measurements, and their performances tested in imaging and dip-pen nanolithography (DPN) writing modes. Wear tests were also conducted to demonstrate the superior behavior of the microfabricated UNCD tips as compared to commercial silicon nitride tips.

2. Results and Discussion

2.1. The Molding Method for UNCD Probes

Molding is well known as a fabrication method for ultrasharp tips of a large variety of materials,[27,28] including diamond,[29] for which tip radii of 30 nm have been reported.[30]

Table 1. Characteristics of different diamond film species.

	Microcrystalline diamond (MCD)	Nanocrystalline diamond (NCD)	Ultrananocrystalline diamond (UNCD)	Diamond-like carbon (DLC)	
				ta-C	ta-H:C
Growth species	CH_3* (H^0)	CH_3* (H^0)	C_2	C	C
Crystallinity	columnar	mixed diamond and nondiamond	equiaxed diamond	mixed diamond and amorphous	amorphous
Grain size	$\approx$0.5–10 μm	50–100 nm	2–5 nm	variable	–
Surface roughness	400 nm–1 μm	50–100 nm	20–40 nm	5–100 nm	1–30 nm
Electronic bonding character	sp^3	up to 50% sp^2 (secondary phase)	2–5% sp^2 (grain boundary)	up to 80% sp^3	up to $\approx$40% sp^3
Hydrogen content	<1%	<1%	<1%	<1%	15–60%

However, the reports on diamond molding did not include oxidation sharpening as an option for increased sharpness of the probes. Tip radii were limited by the geometrical precision of the pyramidal pit etched into silicon, and by the diamond deposition and seeding parameters. The ultimate shape of such a pyramidal pit in Si(100) is given by many factors, which include the accuracy of crystallographic orientation/alignment, and the lithographic performances in providing optimum geometries for windows in the masking layer used for pyramidal etching. A slight increase in the window size in one direction results in the formation of a line-edge probe rather than a point-tip probe. The alignment, lithography, and etching processes are never perfect to the nanometer scale, therefore one expects line-edge probes to be always obtained, depending on how much magnification is used in observing the tip end. In our approach, besides a sufficiently rigorous lithography (± 0.1 μm) and care in alignment (better than $\pm 1°$ for both flat-to-crystal and mask-to-flat alignment), we added an oxidation sharpening step (Figure 1). This step, as well as the additional sharpening due to constraints in the oxide growth in pyramidal pits,[27] performed well in leading to single-point tip geometries.

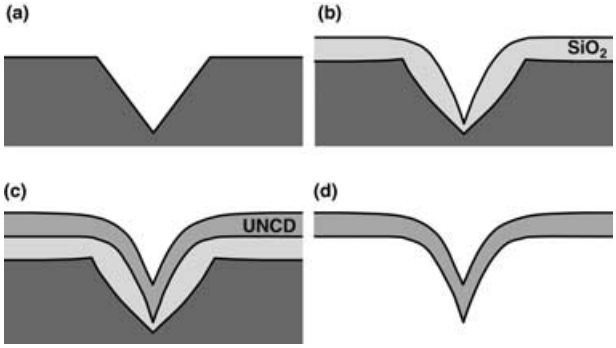

Figure 1. Molding of UNCD by a) forming a pyramidal pit in Si(100) by orientation-dependent etching, b) oxidation sharpening, c) deposition of UNCD, and d) removal of the Si and SiO_2 mold by chemical etching.

The molding method has the general inconvenience that the tip is fabricated facing toward the substrate, thus requiring some microfabrication effort to reverse the probe cantilevers with respect to the handling chip body. Several methods have been reported for reversing the diamond tips, including: 1) building of a chip body by micromachining and gluing of a complementary silicon or glass wafer onto the tip-fabrication wafer;[23] 2) fabricating tips and portions of the cantilevers on one wafer and gluing them onto cantilevers fabricated on other wafers (eventually, made of other materials), followed by releasing.[31] These methods require aligned bonding procedures and a good resistance of the glue joint during the chip release and operation processes. To simplify this sequence, we investigated the use of metal electroforming to build a chip body within an SU-8 photoresist mold, followed by release through dissolution of the silicon substrate. Bonding of a complementary wafer for the chip body has the advantage of offering a medium to develop electronic circuitry without interfering much with tip fabrication, but it is an unnecessary effort in the case of simple conductive probes. In our approach, simple sensors/actuators in film form, such as piezoactuators or piezoresistors, can still be integrated on top of the diamond by proceeding from the mold-side silicon wafer. Additional pre-

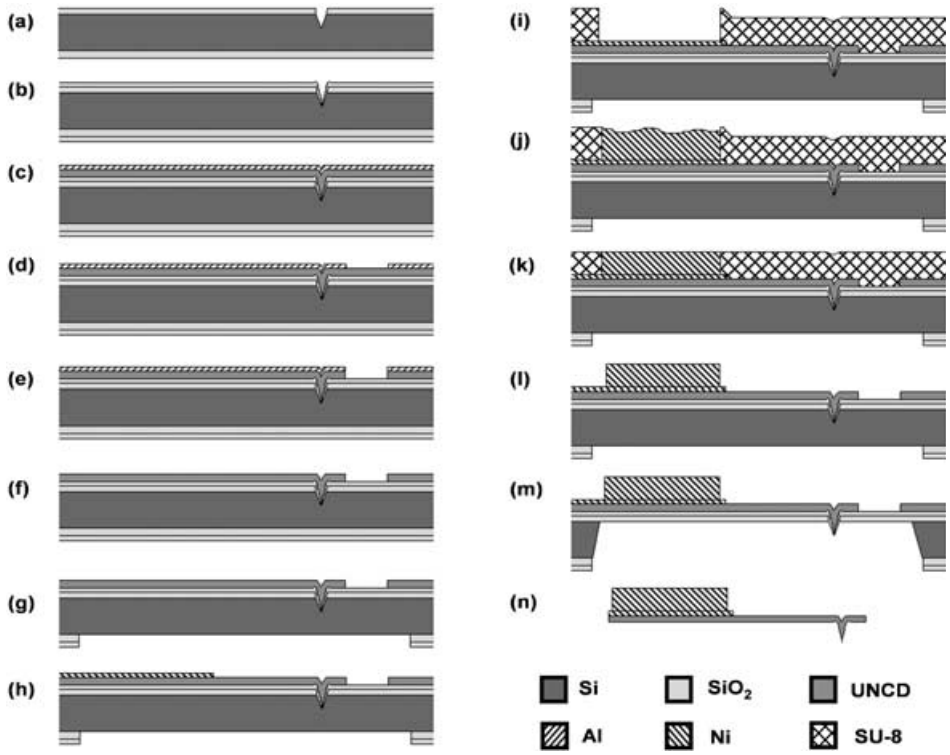

Figure 2. Fabrication of UNCD probes—processing sequence. a) Oxide growth followed by lithography with mask M1, and then etching in KOH solution. b) Oxidation sharpening. c) UNCD and Al deposition. d) Lithography (mask M2) followed by Al etching. e) UNCD etching using RIE. f) Al removal. g) After lithography (mask M3), oxide etching on the back side. h) Ti/Ni deposition followed by patterning (mask M4). Ti layer (not shown in the figure) used as an adhesion layer between UNCD and Ni. i) SU-8 spin-coating and patterning (mask M5). j) Ni electroforming. k) Lapping/polishing. l) SU-8 removal. m) Etching in KOH solution. n) Oxide etching.

NANO MICRO small

cautions in protecting them during removal of the silicon mold may be required.

The processing steps we employed to fabricate molded UNCD probes are summarized in Figure 2. The fabrication started with the formation of an oxide mask (thermal oxidation, 500 nm), which was patterned lithographically by mask M1 with square openings (12×12 μm), followed by KOH (30%, 80°C) etching of pyramidal pits in the Si(100) wafer. Several groups of different size squares and rectangles were fabricated simultaneously with mask M1, which corresponded to different alignment marks, such that a large variety of tip geometries could be obtained. A thermal oxidation sharpening process at 900°C followed, which resulted in a SiO_2 layer >1 μm in thickness on the {100} surface of the Si wafer. Figure 3 shows one sharpened pyramidal mold that exhibits a central black area corresponding to the recessed (sharpened) zone. An ultrasonic seeding procedure was applied with a 4–6-nm-grain diamond powder suspended in methanol (5 mg L^{-1}), to which the wafers were exposed for 30 min and rinsed with isopropanol, then ultrasonically cleaned in methanol for 5 min and dried. Growth of the UNCD layer (0.5–1 μm thick) was achieved by MPCVD in a methane–argon gas mixture, which also contained nitrogen in the case of the N-doped films.[24] Next, an Al mask (80 nm) was deposited by electron-beam evaporation and patterned with mask M2, which defined the cantilevers. The pattern was transferred into UNCD by reactive ion etching (RIE) with an oxygen plasma (30 mTorr, 50 sccm, 200 W), according to a process described in ref. [32], after which the Al mask was removed by wet chemical etching. The oxide on the back side was patterned with mask M3, for subsequent release of the structures. A top metal was then deposited by electron-beam evaporation and patterned on the front side, to form a plating base for the subsequent electroforming of the chip body.

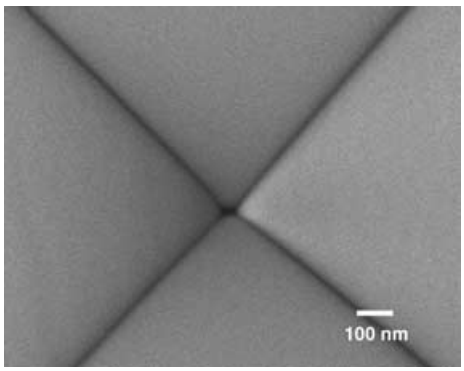

Figure 3. Image of an anisotropically etched pyramidal hole, after sharpening by thermal oxidation.

The plating base metal has to suit the electroforming metal, for example, a 150-nm Ni plating base in the case of Ni electroforming, or 10-nm Ti/200-nm Au for electroforming of gold. The choice of the electroforming metal is based on compatibility with the release procedure. Patterning of the plating base layer (mask M4) is required for avoiding the presence of the metal in the area adjacent to cantilevers, where it may result in metal debris adhering to the cantilevers after their release. At the same time, the plating base pattern has to be continuous, for providing electrical contact to all the areas that need to be plated. Optionally, the plating base can be left on the cantilevers, to act as a reflective coating, provided no electroplating will be performed there.

In our process, a negative-tone SU-8 photoresist layer (MicroChem Co., 330 μm thickness) was deposited and patterned with mask M5, to form a mold for the metal handling-chip body. For the samples presented herein, we used gold electroforming, but other metals may be considered for cost reduction (Ni, Cr) or for special applications including piezoactuators, where Pt would be the metal of choice to subsequently grow a piezoelectric layer on top. The electroforming of the gold layer was performed in two steps: it started with the deposition of 3 μm of gold with a neutral pH Techni-gold 25E (Technic Inc.) sulfamate solution,[33] to provide a good adhesion, and continued with the deposition of the thick chip body from a mildly acid pH Neutronex 309 (Enthone-OMI Inc.) bath. Both processes were performed at 40°C, with a current density of 1 mA cm^{-2}. The metal thickness ranged between 250 and 300 μm. The gold roughness and incidental sidewall overplating were removed by mechanical polishing. The SU-8 resist mold was then removed in a piranha solution. The removal of the Si substrate was performed by KOH etching (30%, 80°C), and the remaining oxide was removed by a buffered HF solution (BHF). After the removal of the sacrificial silicon mold, the chips remained suspended on a Si and gold frame, each supported by two bridges from which they could be easily clipped off using tweezers. The chips containing the UNCD tip/cantilever structures were ready for mounting in a commercial AFM.

2.2. Characterization of the UNCD Probes

Two types of cantilevers with different designs were fabricated. One featured a high-stiffness triangular cantilever (Figure 4a) and the other a low-stiffness arrow-shaped cantilever (Figure 4b). The length of both cantilevers was 170 μm, while the width of the arrow-shaped cantilever was 12 μm and the width of the arms of the triangular cantilevers was 18.8 μm. The thickness of the diamond (UNCD) was between 0.8 and 1.4 μm, depending on batch and wafer-level deposition nonuniformities. The arrow shape was

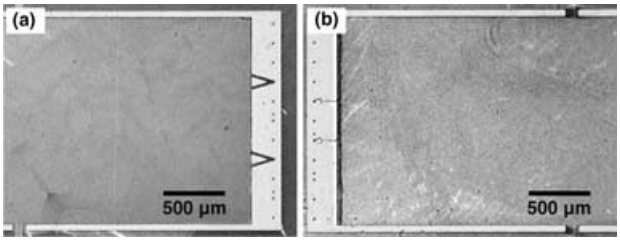

Figure 4. a) High-stiffness triangular cantilevers, placed 600 μm from each other, and b) arrow-shaped cantilevers placed 300 μm from each other. Images after etching the UNCD.

chosen instead of a simple rectangular cantilever to increase the reflective area of the probe near the tip while keeping the stiffness at a minimum. The chip body was of rectangular shape with dimensions 1.6×3.6 mm. Four cantilevers of the same type were placed on each chip, one pair spaced by 300 μm and the other pair spaced by 600 μm on opposite sides of the chips (Figure 4). This design follows roughly the geometry of commercial tips (Veeco, Ultralever). A view of the two types of cantilevers is seen in Figure 5, while a zoom-in of the tip apex is shown in Figure 6.

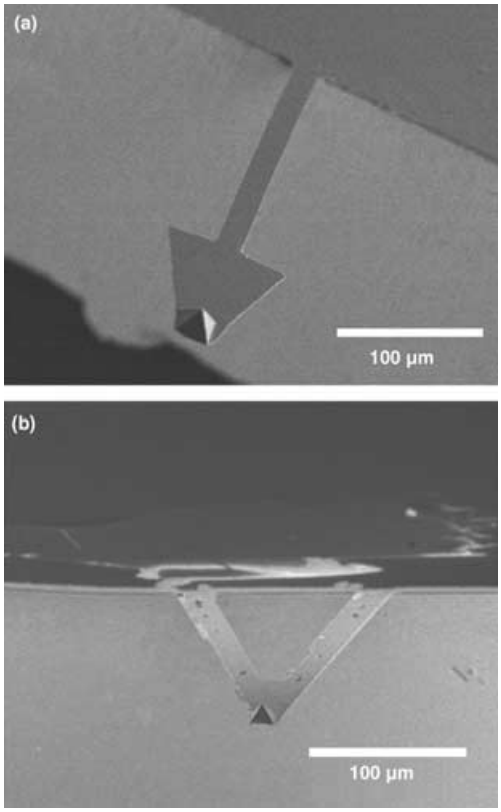

Figure 5. SEM images of the two types of UNCD cantilevers with tips: a) arrow shape, b) triangular cantilevers.

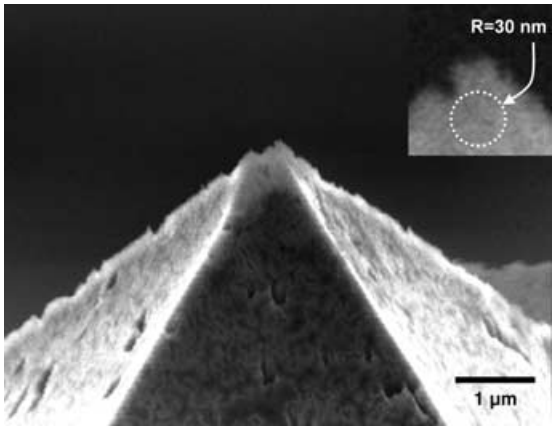

Figure 6. Detail of the tip in Figure 5, with inset showing the apex and a 30-nm-radius circle for reference. The 2–5-nm-scale grain size makes us believe that ultimately, the tip vertex is much sharper.

The tips were characterized and sorted using field-emission scanning electron microscopy (SEM). The high conformality of the UNCD deposition enabled a good coverage of the pyramidal pits used as molds, which resulted in tips with a nanometer-scale apex. In most cases very sharp tips were achieved from protruding features (Figure 6). Due to the nanoscale grain size (2–5 nm) of the material, the ultimate tip radius could be in the 2–5 nm range.

Examination of the UNCD surface morphology reveals that film growth is achieved from seeding nanoparticles, which leads to clustering. As discussed in the context of UNCD strength,[34,35] a large number of grains are present in each cluster and imperfections between clusters were observed in the form of voids.[34,35] In the pit area, larger voids are clearly visible between grain clusters (Figure 6). Growth of UNCD on ultrasonically seeded SiO_2 is more challenging than growth on Si; hence, cluster and void sizes generally tend to increase. Similar structures, but made of crystalline grains, have been observed in MCD films grown on sidewalls of pyramidal pits in Si.[30] The nucleation of MCD grains and intergrain gap formation on tilted surfaces were linked by Scholtz et al.[30] to the size of the diamond particles used in the ultrasonic seeding process. In their experiments, ultrasonic abrasion with 40-μm-diameter diamond particles produced minimal intergrain gaps on flat surfaces, while for pyramidal holes, the optimum diamond particle size for uniform coverage was found to be 1 μm. In our case, the role of film growth is taken by the diamond nanoparticles used in the seeding step, but the nucleation and growth obeys similar rules. The inset of Figure 6 is a zoom-in view of one of the top clusters. A coral-like surface morphology is observed.

The surface roughness of UNCD films can be minimized to values in the 4–7 nm rms range by depositing a very thin (5–10 nm) metallic layer, for example W, Mo, or other carbide-forming material, as nucleation promoter. We found that SiO_2 is a more difficult nucleation medium than Si and results in poor UNCD film adhesion, especially in the case of doped UNCD. Nonetheless, it is indispensable for maximum sharpening. In a variant of the processing sequence, we used an additional lithography step to selectively remove the oxide prior to the UNCD deposition from all areas, except the pyramidal pits. For this purpose, mask M1 was realigned, but using a reversible (negative) photoresist (Shipley AZ5214E), through which the oxide was removed in buffered oxide etch (BOE).

The stiffness of the UNCD cantilevers was measured by the cantilever deflection method, using an AFM probe after calibration with a reference cantilever of known stiffness. We measured a stiffness value of $3.6\ N\,m^{-1}$ for a 1.2-μm-thick triangular cantilever, and a stiffness of $0.94\ N\,m^{-1}$ for a 0.9-μm-thick arrow-shaped cantilever. Knowing the geometry of the cantilever, we could deduce a value of 923 ± 50 GPa for the Young's modulus of UNCD, which correlates well with the value of 960 ± 60 GPa measured by membrane deflection experiments.[25] The stiffness of the arrow-shaped cantilever is close to that of one of the triangular nitride

small NANO MICRO

cantilevers of a commercial nitride probe (tip A of Veeco Si_3N_4 contact-mode probes, $0.58\,N\,m^{-1}$). This information was used to perform a comparative test on the wear resistance of the tips. For this purpose, a Digital Instruments 3100 AFM was used for repeated scanning in contact mode. Imaging of a UNCD surface, $10\times10\,\mu m$ in area, was performed with a constant force of 30 nN. The scanning of the UNCD tip was performed on the surface of a UNCD film deposited on Si for the purpose of accelerating the wear tests. The tests were run for UNCD and Si_3N_4 tips. The tips were imaged before and after the test using a field-emission SEM (LEO Gemini 1525). After one hour of scanning, the nitride tips showed visible wear, while the UNCD tips showed no appreciable change (Figure 7). The degradation of the silicon nitride tip could also be detected in the quality of topographic AFM images, while the images recorded with the UNCD tip showed no appreciable change.

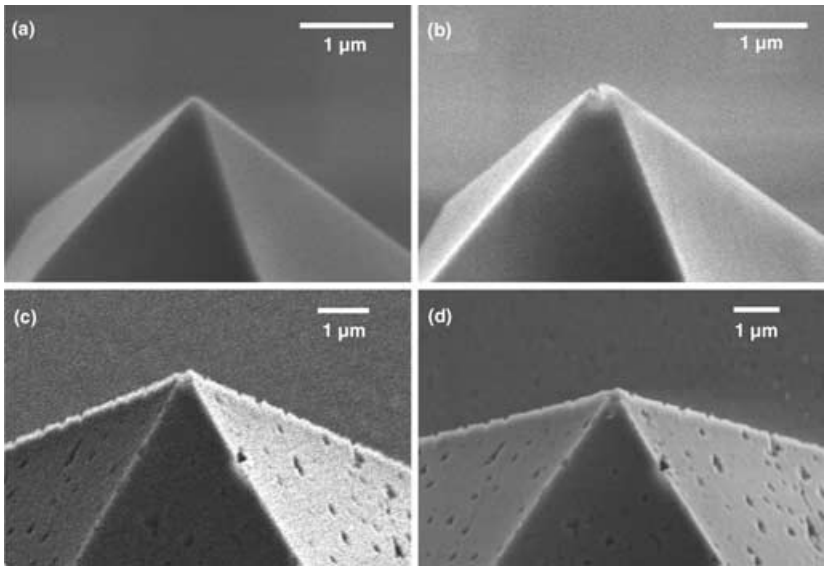

Figure 7. Si_3N_4 tip before (a) and after (b) the wear test, showing damage. UNCD tip before (c) and after (d) the same test, showing no visually detectable damage.

In an attempt to find the dominant wear mechanisms in UNCD, we looked for changes in the diamond tip after long scans performed for 3 h with an increased constant force of 50 nN using the triangular-shaped UNCD cantilever. Figure 8 presents a view of the tip apex before and after the wear experiment. One can notice the absence of a relatively large portion of the tip apex and debris gathered on the sidewalls of the pyramid. The geometry of the worn tip suggests that the observed wear seems to be controlled by dislodgment of a cluster of UNCD grains as a result of intercluster cracking, rather than by atom-by-atom removal at the atomic scale. This finding shows that to increase the wear resistance of UNCD probes, one has to optimize the intercluster strength or eliminate the formation of clusters. The role of seeding in UNCD surface morphology and strength is discussed in refs. [25,35]. The elimination of clustering would also have a positive impact in obtaining smoother, high-conformity filling of the mold template with diamond, thus resulting in sharper tips with controlled geometry at the nanoscale. Research on optimization of seeding and deposition parameters is under way and will be reported in a future manuscript.

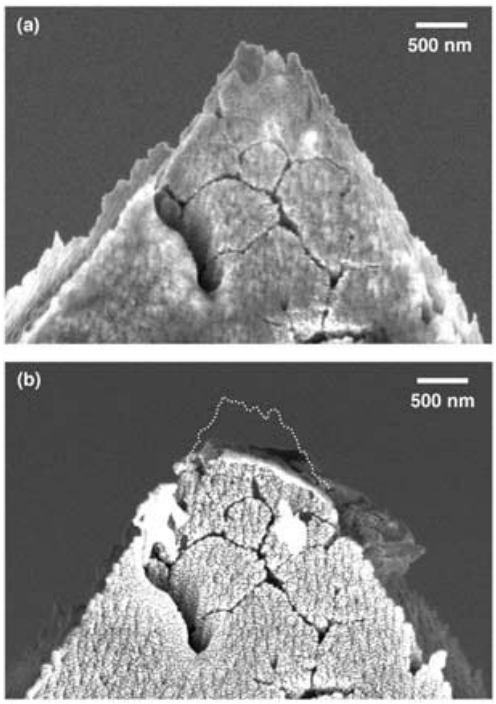

Figure 8. High-resolution SEM image of a UNCD tip before (a) and after (b) a prolonged wear test. The absence of portions of the material roughly following the intercluster contour line suggests that failure happens mainly by detaching of clusters, rather than by continuous smooth wear.

A vibration test on the arrow-shaped UNCD cantilevers was performed using a Polytec vibrometer in differential interferometric mode (the reference beam on the chip body and the measuring beam on the cantilever). The first three resonant frequencies were measured at 32.2, 52.31, and 53.94 kHz, respectively (movies are provided as supporting material[36]). The first and the last vibration frequencies correspond to vibration modes in which the pyramid axis oscillates with rotation around the perpendicular to the chip surface. The intermediate frequency corresponds to a motion in which the pyramid axis oscillates without rotation, that is, it remains perpendicular to the chip surface during the whole motion. This vibration mode is well-suited for AFM

techniques involving cantilever oscillations perpendicular to the surface being scanned (tapping mode).[37] Note that the high stiffness achievable with UNCD cantilevers makes it possible to increase the working frequencies, with obvious benefits in sensitivity and resolution.

2.3. AFM Imaging and DPN Tests

The performance of the UNCD AFM probes is illustrated by DPN writing and lateral-force friction measurements. For DPN, the UNCD tip was dipped into a 10% mercaptohexanoic acid (MHA) solution in acetonitrile, dried, and mounted on the AFM head (Digital Instruments 3100). Writing was performed on the surface of a freshly deposited gold thin film (100 nm Au electron-beam-evaporated onto a microscope glass slide) with in-house-developed software.

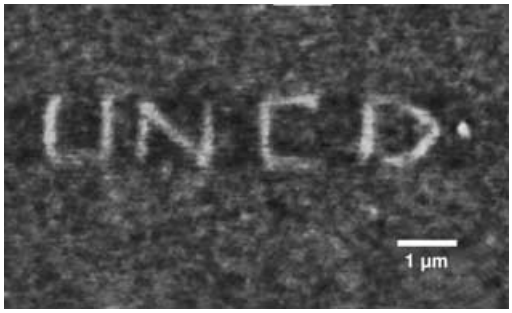

Figure 9. "UNCD" written with MHA on a freshly deposited gold film using a UNCD triangular-shaped probe. The line width is 200 nm. Imaging of the MHA pattern was performed with the same UNCD tip in lateral force mode.

Writing of the letters U-N-C-D with the molecular ink was achieved with a line width of about 200 nm (Figure 9).

The writing speed, which is controlled by the rate of molecular diffusion, was compared between the UNCD arrow-shaped and commercial nitride tips by performing static contact depositions of MHA dots on Au, with contact times of 5, 10, and 20 seconds. Both experiments were run under

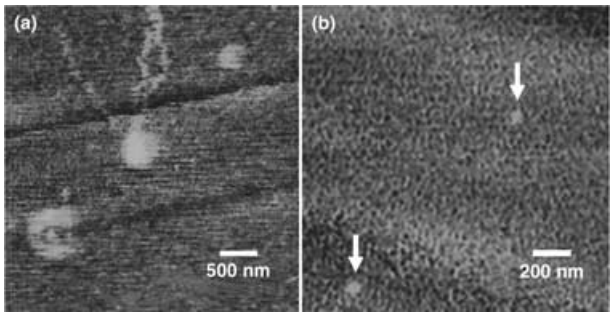

Figure 10. a) Three MHA dots on gold, obtained by contacting the surface for 5, 10, and 20 s with the arrow-shaped UNCD probe (from top right to bottom left). The image was recorded with the same probe in lateral force imaging mode. The diameters of the dots are 360, 540, and 710 nm, respectively. b) These 80-nm-diameter dots are the best-resolved features obtained so far.

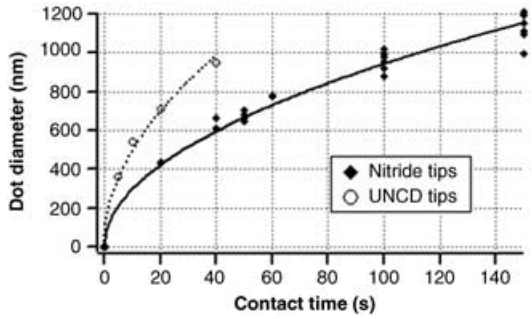

Figure 11. Graph showing the diameter of the MHA dots obtained with UNCD and Si_3N_4 tips in similar mode, as a function of contact time. Continuous fits were made as square root functions $Y=At^{1/2}$, and showed a good agreement with the model of Jang et al.[4]

similar conditions (contact force 50 nN, humidity 50±5%, temperature 23 °C). The results are shown in Figures 10 and 11. The UNCD tips showed a slightly faster deposition rate, but within the limits of variability encountered among different nitride tips. This result is consistent with the wetting properties of diamond, which is slightly more hydrophilic than silicon nitride. The smallest features we could write so far with UNCD tips, by using the DPN technique, were 80-nm-diameter dots (Figure 10b).

The imaging of the DPN-deposited dots and letters was performed in all cases with the same tips used for deposition by running the instrument in frictional force mode. This procedure also demonstrates that the developed UNCD probes produce high-quality frictional force AFM images.

Experiments conducted in our laboratory also showed that the UNCD tips can be used to write by scratching the relatively soft gold surface. In this continuous writing mode, the tip is moved between a discrete number of points while keeping it in contact mode at relatively high contact force. The result of such a scratch test is shown in Figure 12.

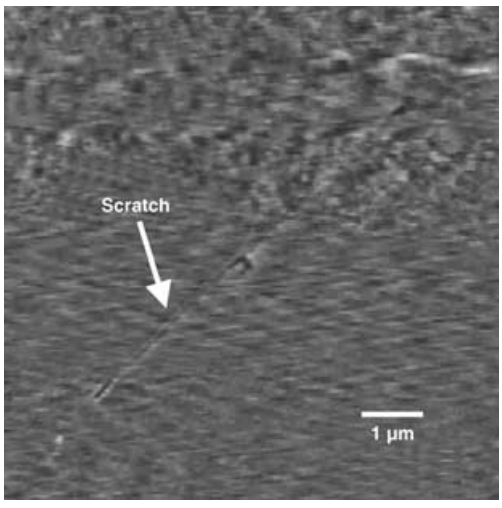

Figure 12. AFM topography image of a scratch on a gold surface obtained by translating a UNCD tip in contact mode between two specified points.

NANO MICRO small

3. Conclusions

Sharp UNCD probes were fabricated by molding into oxidation-sharpened pyramidal pits etched in silicon together with metal electroforming to build the handling chip. SEM imaging indicated that the UNCD tips have radii of about 30 nm. The UNCD cantilevers and tips were characterized by SEM (for geometry), AFM deflection (for stiffness), and optical interferometric vibrometer (for resonant frequencies). A preliminary wear test was performed, which showed that the UNCD probes exhibit a far superior performance to that of currently available commercial silicon nitride tips. The wear mechanism of the monolithic UNCD tips appears to be dominated by detaching of grain clusters from the tip rather than by atomic-scale erosion of surface atoms. Research on optimization of seeding and deposition parameters is currently under way to further exploit the full potential of UNCD as a material for producing high-stiffness, low-wear monolithic tips for AFMs or large tip arrays for massive parallel fabrication of large arrays of nanostructures.

We demonstrated the feasibility of achieving superior AFM contact-mode imaging, DPN writing with MHA molecules on gold substrates, and lateral-force-mode imaging by using UNCD monolithic tips. Resolution and writing performances similar to those obtained with commercial silicon nitride tips were obtained. Furthermore, we showed that the probe material and fabrication technique are particularly suitable for integration in one- and two-dimensional arrays of probes.

Acknowledgement

This work was sponsored by the National Science Foundation NIRT project No. CMS00304472 and in part by the Nanoscale Science and Engineering Initiative of the National Science Foundation under NSF Award Number EEC-0118025. The ANL authors also acknowledge the continuous support of the U.S. DOE Office of Science—Basic Energy Science/Materials Science & Engineering under Contract No. W-31-109-ENG-38. We thank Professors Mark Hersam and Chad Mirkin for many insightful discussions. The authors acknowledge the Microfabrication Applications Laboratory (MAL) of the University of Illinois at Chicago, the Materials Processing and Crystal Growth Facility (MPCGF) of Northwestern University, Northwestern University Atomic and Nanoscale Characterization Experimental Center (NUANCE), and the Microfabrication Center of Argonne National Laboratory for access to their fabrication and characterization facilities. The authors thank Dr. R. Divan from Argonne National Laboratory for assistance in thick-resist molding and electroforming processes.

[1] R. D. Piner, J. Zhu, F. Xu, S. Hong, C. A. Mirkin, *Science* **1999**, *283*, 661 – 663.
[2] P. E. Sheehan, L. J. Whitman, W. P. King, B. A. Nelson, *Appl. Phys. Lett.* **2004**, *85*, 1589 – 1591.
[3] Y. Li, B. W. Maynor, J. Liu, *J. Am. Chem. Soc.* **2001**, *123*, 2105 – 2106.
[4] J. Jang, S. Hong, G. C. Schatz, M. A. Ratner, *J. Chem. Phys.* **2001**, *115*, 2721 – 2729.
[5] K.-H. Kim, N. Moldovan, H. D. Espinosa, *Small* **2005**, *1*, 632 – 635.
[6] C. Mine, S. R. Manalis, C. F. Quate, *Bringing Scanning Probe Microscopy up to Speed*, Kulver Academic Publishers, Boston, **1999**, p. 119.
[7] M. Zhang, D. Bullen, S.-W. Chung, S. Hong, K. S. Ryu, Z. Fan, C. A. Mirkin, C. Liu, *Nanotechnology* **2002**, *13*, 212 – 217.
[8] P. Vettiger, M. Despont, U. Drechsler, U. Durig, W. Haberle, M. I. Lutwyche, H. E. Rothuizen, R. Stutz, R. Widmer, G. K. Binnig, *IBM J. Res. Dev.* **2000**, *44*, 323 – 340.
[9] V. B. Kley, US Patent US6 353 219 B1, Mar. 5, **2002**.
[10] T. Leinhos, M. Stopka, E. Oesterschulze, *Appl. Phys. A* **1998**, *66*, S65 – S69.
[11] E. Meyer, H. J. Hug, R. Bennewitz, *Scanning Probe Microscopy: The Lab on a Tip*, Springer, Berlin, **2004**.
[12] R. P. Lu, K. L. Kavanagh, St. J. Dixon-Warren, A. J. Spring Thorpe, R. Streater, I. Calder, *J. Vac. Sci. Technol. B* **2002**, *20*, 1682 – 1689.
[13] M. C. Hersam, A. C. F. Hoole, S. J. O'Shea, M. E. Welland, *Appl. Phys. Lett.* **1998**, *72*, 915 – 917.
[14] Veeco, *Application Modules: Dimension and MultiMode Manual*, chap. 2, **2003**.
[15] A. S. Basu, S. McNamara, Y. B. Gianchandani, *J. Vac. Sci. Technol. B* **2004**, *22*, 3217 – 3220.
[16] M. A. Angadi, T. Watanabe, A. Bodapati, X. Xiao, O. Auciello, J. A. Carlisle, J. A. Eastman, P. Keblinski, P. K. Schelling, S. R. Phillpot, *Nat. Mater.* **2005**, submitted.
[17] T. Hantschel, P. Niedermann, T. Trenkler, W. Vandervorst, *Appl. Phys. Lett.* **2000**, *76*, 1603 – 1605.
[18] Ph. Niedermann, W. Hänni, N. Blanc, R. Christoph, J. Burger, *J. Vac. Sci. Technol. A* **1996**, *14*, 1233 – 1236.
[19] R. Kaneco, S. Oguchi, *Jpn. J. Appl. Phys.* **1990**, *29*, 1854 – 1855.
[20] E. P. Visser, J. W. Gerritsen, W. J. P. van Encevort, H. van Kempen, *Appl. Phys. Lett.* **1992**, *60*, 3232 – 3234.
[21] R. Rameshan, *Thin Solid Films* **1999**, *340*, 1 – 6.
[22] T. A. Friedmann, J. P. Sullivan, J. A. Knapp, D. R. Tallant, D. M. Follstaedt, D. L. Medlin, P. B. Mirkarimi, *Appl. Phys. Lett.* **1997**, *71*, 3820 – 3822.
[23] C. Mihalcea, W. Scholz, A. Malave, D. Albert, W. Kulisch, E. Oesterschulze, *Appl. Phys. A* **1998**, *66*, S87 – S90.
[24] A. R. Kraus, O. Auciello, D. M. Gruen, A. Jayatissa, A. Sumant, J. Tucek, D. C. Mancini, N. Moldovan, A. Erdemir, D. Ersoy, M. N. Gardos, H. G. Busmann, E. M. Meyer, M. Q. Ding, *Diamond Relat. Mater.* **2001**, *10*, 1952 – 1961.
[25] a) H. D. Espinosa, B. C. Prorok, B. Peng, K.-H. Kim, N. Moldovan, O. Auciello, J. A. Carlisle, D. M. Gruen, D. C. Mancini, *Exp. Mech.* **2003**, *43*, 256 – 268; b) H. D. Espinosa, B. Peng, B. C. Prorok, N. Moldovan, O. Auciello, J. A. Carlisle, D. M. Gruen, D. C. Mancini, *J. Appl. Phys.* **2003**, *94*, 6076 – 6084.
[26] A. Erdemir, C. Bindal, G. R. Fenske, C. Zuiker, R. Csencsits, A. R. Krauss, D. M. Gruen, *Diamond Relat. Mater.* **1996**, *6*, 31 – 47.
[27] P. N. Minh, O. Takahito, E. Masayoshi, *Fabrication of Silicon Microprobes for Optical Near-Field Applications*, CRC Press, Boca Raton, FL, **2002**, chap. 4.
[28] J. Zou, X. Wang, D. Bullen, K. Ryu, C. Liu, C. A. Mirkin, *J. Micromech. Microeng.* **2004**, *14*, 204 – 211.
[29] K. Okano, K. Hoshina, M. Iida, S. Koizumi, T. Inuzuka, *Appl. Phys. Lett.* **1994**, *20*, 2742 – 2744.
[30] W. Scholtz, D. Albert, A. Malave, S. Werner, C. Mihalcea, W. Kulisch, E. Oesterschulze, *Proc. SPIE* **1997**, *3009*, 61 – 71.
[31] Ph. Niedermann, W. Hänni, D. Morel, A. Perret, N. Skinner, P.-F. Indermühle, N.-F. de Rooij, P.-A. Buffat, *Appl. Phys. A* **1998**, *66*, S31 – S34.

[32] N. Moldovan, O. Auciello, A. V. Sumant, J. A. Carlisle, R. Divan, D. M. Gruen, A. R. Krauss, D. C. Mancini, A. Jayatissa, J. Tucek, *Proceedings of the SPIE 2001 International Symposium on Micromachining and Microfabrication*, San Francisco, CA, October 22 – 25, **2001**, *4557*, 288 – 298.
[33] Techni-gold 25E, Technic Inc., Cranston, RI, http://www.technic.com.
[34] B. Peng, H. D. Espinosa, *Proceedings of the 2004 ASME International Mechanical Engineering Congress*, CA, November 13 – 19, **2004**.
[35] H. D. Espinosa, B. Peng, B. C. Prorok, N. Moldovan, O. Auciello, J. A. Carlisle, X. Xiao, D. M. Gruen, D. C. Mancini, *J. Appl. Phys.* **2005**, submitted.
[36] http://clifton.mech.northwestern.edu/≈espinosa/publications/movielink.htm
[37] F. J. Giessibl, *Rev. Mod. Phys.* **2003**, *75*, 949 – 983.

Received: January 24, 2005

